Journal of Zhejiang University SCIENCE A
ISSN 1673-565X (Print); ISSN 1862-1775 (Online)
www.zju.edu.cn/jzus; www.springerlink.com
E-mail: jzus@zju.edu.cn

Low-cost sensorless control of four-switch, brushless DC motor drive with direct back-EMF detection

Abolfazl HALVAEI NIASAR[†1,2], Abolfazl VAHEDI[2], Hassan MOGHBELLI[3]

([1]*Department of Electrical Engineering, Faculty of Engineering, University of Kashan, Kashan 87317-51167, Iran*)

([2]*Center of Excellence for Power System Automation and Operation, Iran University of Science and Technology, Tehran 16846-13114, Iran*)

([3]*Department of Science and Mathematics, Texas A&M University at Qatar, Doha 23874, Qatar*)

[†]E-mail: halvaei@kashanu.ac.ir

Received Feb. 4, 2008; Revision accepted May 11, 2008; Crosschecked Nov. 10, 2008

Abstract: We propose a position sensorless control scheme for a four-switch, three-phase brushless DC motor drive, based on the zero crossing point detection of phase back-EMF voltages using newly defined error functions (EFs). The commutation instants are 30° after detected zero crossing points of the EFs. Developed EFs have greater magnitude rather than phase or line voltages so that the sensorless control can work at a lower speed range. Moreover, EFs have smooth transitions around zero voltage level that reduces the commutation errors. EFs are derived from the filtered terminal voltages v_{ao} and v_{bo} of two low-pass filters, which are used to eliminate high frequency noises for calculation of the average terminal voltages. The feasibility of the proposed sensorless control is demonstrated by simulation and experimental results.

Key words: Brushless DC motor, Four-switch inverter, Sensorless control, Back-EMF voltage sensing, DSP
doi:10.1631/jzus.A0820097 **Document code:** A **CLC number:** TM921

INTRODUCTION

The permanent magnet brushless DC (BLDC) motor is increasingly being used in automotive, computer, industrial and household products because of its high efficiency, high torque, ease of control, and lower maintenance. The BLDC motor is designed to utilize the trapezoidal back-EMF with square wave currents to generate constant torque (Pillay and Krishnan, 1989). Conventional BLDC motor drive is generally implemented via six-switch three-phase inverter and three Hall Effect position sensors that provide six commutation points per electrical cycle. For some applications it is important to reduce the manufacturing cost of the drive. Cost reduction is usually achieved by elimination of the drive components such as power switches and sensors. Effective algorithms should be designed to produce the desired performance. A four-switch inverter topology has been developed and used for three-phase BLDC motor drive recently. Reduction in the number of power switches, DC power supplies, switch driver circuits, and also in losses and the total price, is the main feature of this topology. However, in the four-switch topology, for current regulation, conventional control schemes are not effective. A new and effective current control scheme was proposed in (Lee *et al*., 2003) to obtain 120° rectangular currents based on the independent control of the phase current.

Manufacturing cost of the BLDC motor drive can be reduced more by eliminating position sensors and developing feasible sensorless methods. Furthermore, sensorless control is the only choice for some applications where the sensors cannot function reliably because of the harsh environments. The major sensorless methods published in the literature can be classified as follows (Jahnson *et al*., 1999; Acarnley and Watson, 2006): back-EMF sensing techniques, flux estimation method, stator inductance variations method, observers and intelligent control methods. The sensorless techniques that

utilize the back-EMF voltage include: (1) terminal voltage sensing, (2) third harmonic back-EMF voltage sensing, and (3) freewheeling diode conduction current sensing. Sensorless techniques based on back-EMF and terminal voltages are the most popular due to their simplicity, ease of implementation and lower cost (Shao and Nolan, 2002; Su and McKeever, 2004; Zhou *et al*., 2005). They lead to manufacturing the commercial sensorless integrated circuits (ICs) (Wang *et al*., 2007). Most of the sensorless methods for the six-switch inverter BLDC motor drive are not directly applicable to the four-switch inverter, because in this inverter topology, they detect less than six commutation points and other commutation instants must be interpolated.

So far, there have been few studies on sensorless control of the four-switch inverter, three-phase BLDC motor drive. Recently, a new sensorless control method has been proposed by Lin *et al*.(2008) for a four-switch topology. Based on experimental results they found that two crossing points between two terminal voltages A and B coincide to two commutation instants and other four commutation instants are attained via interpolation and shift delay software. Also, a new position sensorless estimation based on the line-to-line voltages was presented (Halvaei Niasar *et al*., 2007), in which six commutation points were detected. In spite of its simplicity and low cost, the considerable drop voltage on the stator impedance at low speeds and heavy loads has limited its applications at low speed range. This paper presents a low cost BLDC motor drive using a feasible sensorless method that detects six commutation points (Halvaei Niasar, 2007). The proposed method uses the zero crossing points (ZCPs) of three error functions (EFs). It is shown that the transition of EFs around zero voltage level is smooth enough, which reduces the zero detection error significantly. The validity of the proposed sensorless method is proved via simulation and experiments.

FOUR-SWITCH, THREE-PHASE BLDC MOTOR DRIVE

Fig.1 shows the configuration of a four-switch inverter along with the equivalent circuit of a three-phase BLDC motor. The typical mathematical model of the BLDC motor is represented as follows:

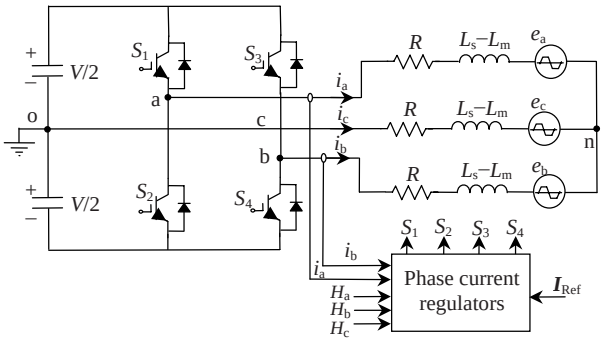

Fig.1 Four-switch brushless DC motor drive and equivalent circuit of brushless DC motor

$$\begin{bmatrix} v_{an} \\ v_{bn} \\ v_{cn} \end{bmatrix} = \begin{bmatrix} R & 0 & 0 \\ 0 & R & 0 \\ 0 & 0 & R \end{bmatrix} \begin{bmatrix} i_a \\ i_b \\ i_c \end{bmatrix} + \begin{bmatrix} e_a \\ e_b \\ e_c \end{bmatrix} + \begin{bmatrix} L_s - L_m & 0 & 0 \\ 0 & L_s - L_m & 0 \\ 0 & 0 & L_s - L_m \end{bmatrix} \frac{\mathrm{d}}{\mathrm{d}t} \begin{bmatrix} i_a \\ i_b \\ i_c \end{bmatrix}, \tag{1}$$

where v_{an}, e_a, i_a, L_s and L_m represent the phase voltage, back-EMF voltage, phase current, self inductance and mutual inductance of phase A, respectively.

The electromagnetic torque is expressed as

$$T_e = \frac{Z_p}{2\omega_m}(e_a i_a + e_b i_b + e_c i_c), \tag{2}$$

where ω_m is the rotor speed and Z_p is the number of magnetic poles.

Fig.2 shows the phase back-EMF and current waveforms, and Hall Effect sensor signals of a three-phase BLDC motor drive in the ideal case. In each operation mode, only two phases are conducting and the third phase is inactive. To drive the motor with maximum and constant torque, the phase currents should be square waves. However, in a four-switch inverter, the generation of 120° conducting current profiles is inherently difficult (Lee *et al*., 2003). Hence, in order to use the four-switch inverter topology for a three-phase BLDC motor, the direct phase current (DPC) control approach is used. By this way, the currents of phases A and B in two modes II and V are controlled via independent current regulators. Therefore, the back-EMF voltage of phase C cannot cause current distortion in the phases A and B.

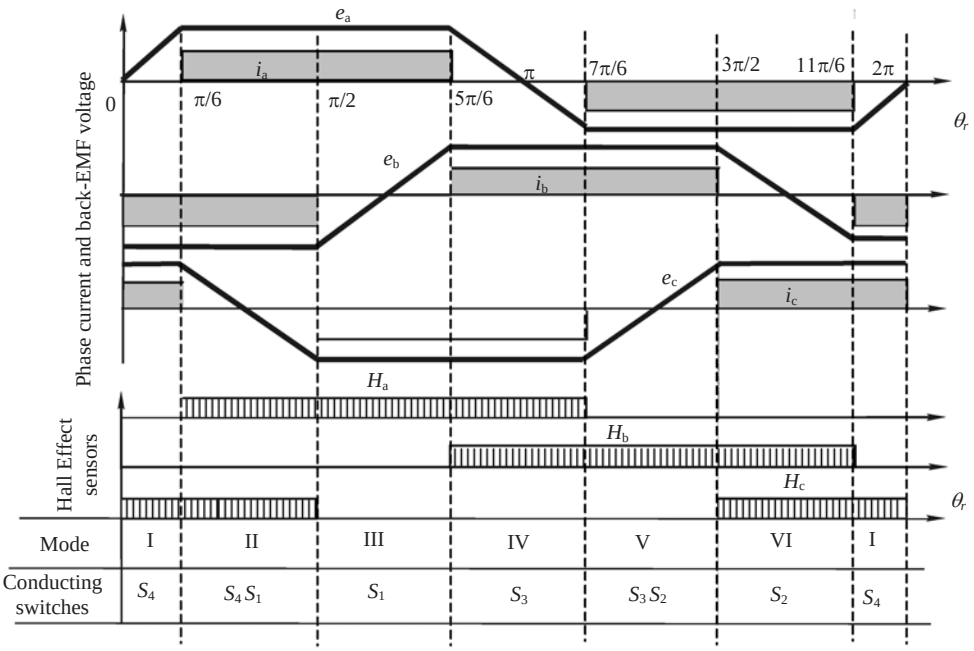

Fig.2 Signal waveforms of the brushless DC motor

SENSORLESS CONTROL OF FSTPI BASED ON ERROR FUNCTIONS

Commutation instants are 30° after ZCPs of phase back-EMF voltages, as shown in Fig.2. But, the stator winding back-EMF voltage is a physical quantity that is hard to measure directly. Therefore, detecting the motor terminal voltage is the normal way to find the zero crossing points. In this study, three EFs in combination with two terminal voltages (of phases A and B) are developed, in which they are synchronized with phase back-EMF voltages. The terminal voltages of the four-switch inverter BLDC motor with respect to the middle point of the DC-bus, based on Fig.1, can be expressed as

$$\begin{cases} v_{ao} = Ri_a + L\dfrac{\mathrm{d}i_a}{\mathrm{d}t} + e_a + v_{no}, \\ v_{bo} = Ri_b + L\dfrac{\mathrm{d}i_b}{\mathrm{d}t} + e_b + v_{no}, \\ v_{co} = Ri_c + L\dfrac{\mathrm{d}i_c}{\mathrm{d}t} + e_c + v_{no} = 0. \end{cases} \tag{3}$$

Because only two phases are always energized, the currents of the two phases have the same amplitude and opposite direction, while in the third phase (silent phase), the current is zero. Adding the three equations in Eq.(3), we obtain

$$v_{ao} + v_{bo} = e_a + e_b + e_c + 3v_{no}. \tag{4}$$

According to Fig.2, while any phase back-EMF voltage crosses zero, the summation e_a+e_b+e_c becomes zero, and therefore Eq.(4) can be rewritten as

$$v_{no} = (v_{ao} + v_{bo})/3. \tag{5}$$

Also, for the silent phase with zero current, Eq.(3) results in

$$e_x = v_{xo} - v_{no},\ x = \mathrm{a, b, c}. \tag{6}$$

Therefore, when any back-EMF voltage crosses zero, Eq.(6) results in

$$v_{xo} = v_{no},\quad x = \mathrm{a, b, c}. \tag{7}$$

Substituting Eq.(5) into Eq.(7) results in the following relations at back-EMF zero crossings:

$$v_{ao} = \begin{cases} 0.5v_{bo}, & \text{if } e_a = 0, \\ 2v_{bo}, & \text{if } e_b = 0, \\ -v_{bo}, & \text{if } e_c = 0. \end{cases} \tag{8}$$

Therefore, to detect the ZCPs of the back-EMF voltages, new EFs (EF_x) are defined as

$$\begin{cases} EF_a(v_{ao}, v_{bo}) = v_{ao} - 0.5v_{bo}, \\ EF_b(v_{ao}, v_{bo}) = -v_{ao} + 2v_{bo}, \\ EF_c(v_{ao}, v_{bo}) = -v_{ao} - v_{bo}. \end{cases} \quad (9)$$

Zero crossing detection of EF_a, EF_b and EF_c generates three virtual Hall position signals VH_a, VH_b and VH_c, respectively, which leads to the commutation points 30°. Therefore, to attain to the commutation points, depending on the motor speed, correct delay time should be used. Determination of the EFs and detection of their ZCPs can be implemented via hardware or in software. Table 1 summarizes the relation between virtual Hall sensor signals and corresponding operation modes.

Table 1 Commutation logic with respect to the signs of error functions

Error function	EF_x^+	EF_x^-	Next mode	$H_cH_bH_a$
EF_b	+	–	I	100
EF_a	–	+	II	101
EF_c	+	–	III	001
EF_b	–	+	IV	011
EF_a	+	–	V	010
EF_c	–	+	VI	110

EF_x^+ and EF_x^- denote the signs of EF_x before and after their zero crossing, respectively

SIMULATION RESULTS

The validity of the proposed sensorless technique is proved via some simulations. The BLDC motor is a high-torque, low-speed motor with 16 poles, whose parameters are given in Table 2. Figs.3a and 3b show the voltage, current, and developed virtual Hall sensors waveforms of the sensorless four-switch BLDC motor drive at 35 and 180 r/min, respectively. Average terminal voltages are used to determinate the EFs and corresponding virtual Hall signals. In Section 3, it has been proved that in spite of the phase current value, zero crossings of EFs coincide to zero crossings of back-EMF voltages. Therefore, the load torque does not affect the estimation error in the presented sensorless method, and the phase delay of the filters is the main source of the estimation error. To compensate the phase delay caused by low-pass filters, virtual Hall signals are delayed less than 30°.

Table 2 Brushless DC motor parameters

Parameter	Value	Parameter	Value
P_n (W)	425	Z_p (pole)	16
T_n (N·m)	10	ω_n (r/min)	350
R (Ω)	0.64	J (kg·m^2)	5E−4
L_s (mH)	1.0	M (mH)	0.25
K_t (N·m/A)	1.194	K_e (V·min/r)	0.0667

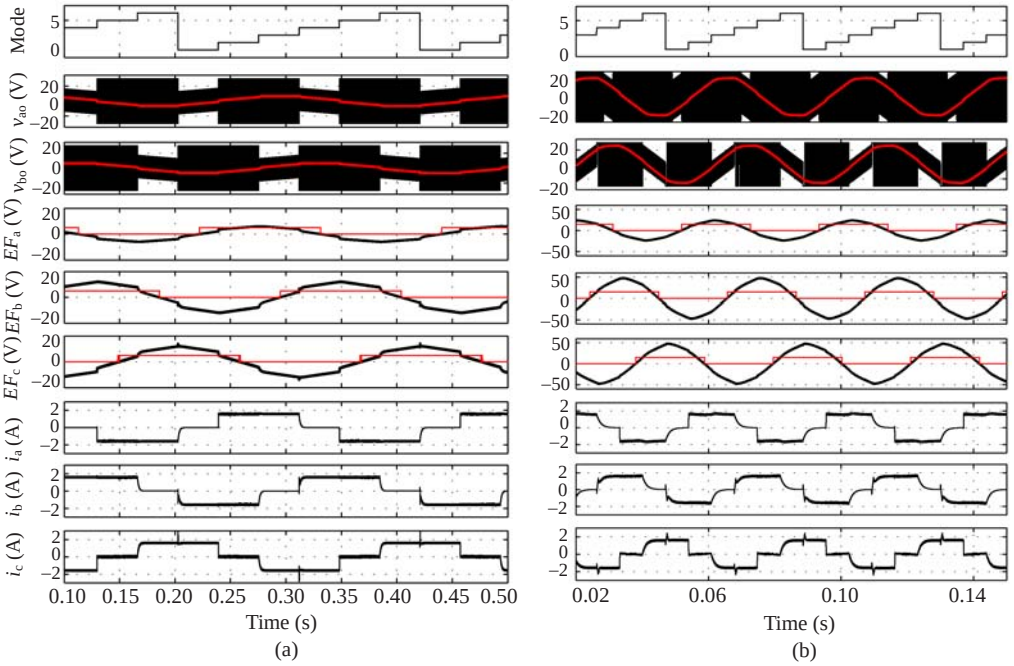

Fig.3 Waveforms of terminal voltages, error functions, and phase currents of the developed sensorless method at 35 r/min (a) and 180 r/min (b)

EXPERIMENTAL RESULTS

Fig.4 shows the experimental setup designed and developed in our laboratory. The system was controlled via a DSP controller TMS320LF2407A (Texas Instruments, 2001). Determination of the EFs and detection of their zero crossing points were carried out via hardware. Terminal voltages were PWM signals and the design of the proper filters is important for calculation of their average values as well as detection of zero crossings (Li *et al.*, 2006). In this study, two second-order Butterworth low-pass filters are designed with the pass-band frequency of 140 Hz (with −0.1 dB attenuation). The phase delay of the filters at 50 r/min (6.5 Hz) and 250 r/min (35 Hz) are 1° and 4°, respectively, which are negligible phase delays for low cost applications.

Fig.5 shows the measured phase back-EMF voltages. Rising edge of position signal H_a is simultaneous with the flat part of back-EMF voltage e_a.

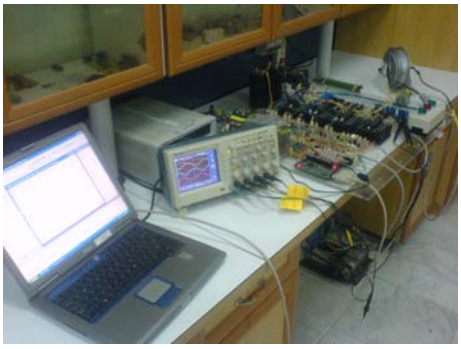

Fig.4 Experimental setup of the sensorless brushless DC motor drive system

Fig.6 shows the instantaneous and the filtered terminal voltages at low and high speeds. The voltage scale of the voltage transducers is 21 V/V. At high speeds and in modes II and V, due to the higher applied voltage to the motor, there is some switching on the terminal voltage. The switchings of phases A and B are different because they come from independent current regulators. The filtered voltages are used to make the EFs.

Figs.7a and 7b show the EFs at 60 and 210 r/min, respectively. The error function EF_a has the lower magnitude rather than EF_b and EF_c, which confirms the simulation results in Fig.3.

Fig.8 shows the corresponding virtual Hall position signals that are made from zero crossing detection of the error functions. They are 30° in advance to the physical Hall Effect sensors. Therefore, 30° phase delay is implemented to predict the

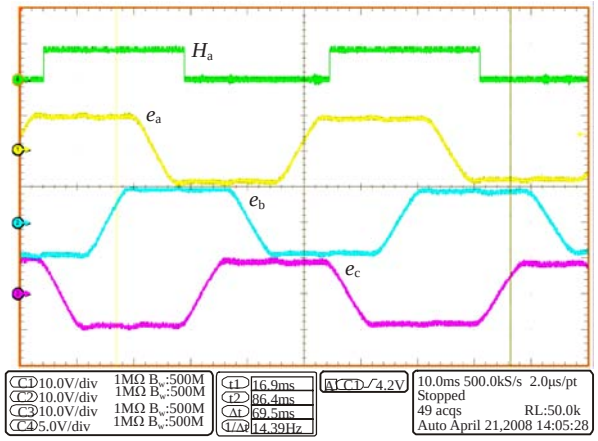

Fig.5 Measured back-EMF voltages of brushless DC motor

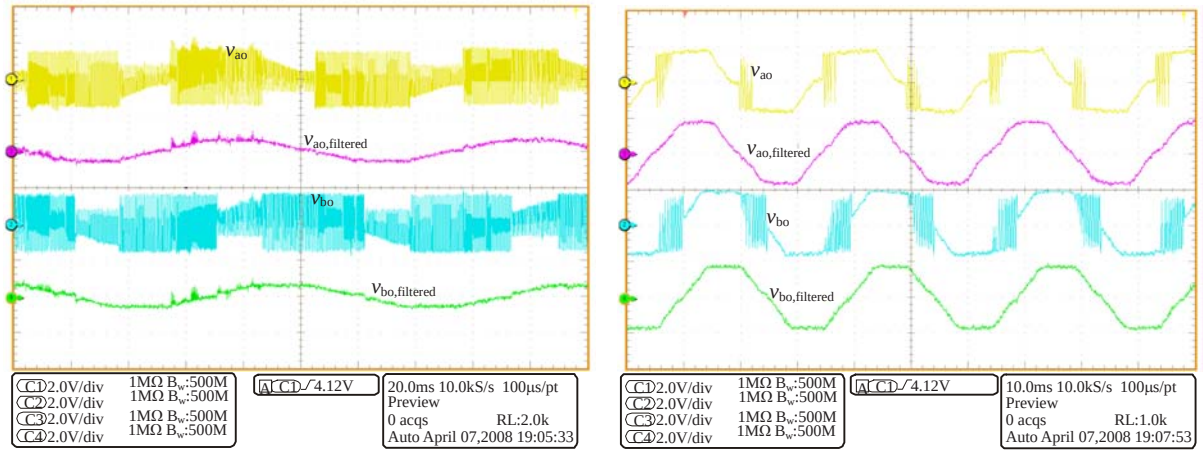

(a) (b)

Fig.6 Measured instantaneous and filtered terminal voltages v_{ao} and v_{bo} at 60 r/min (a) and 250 r/min (b)

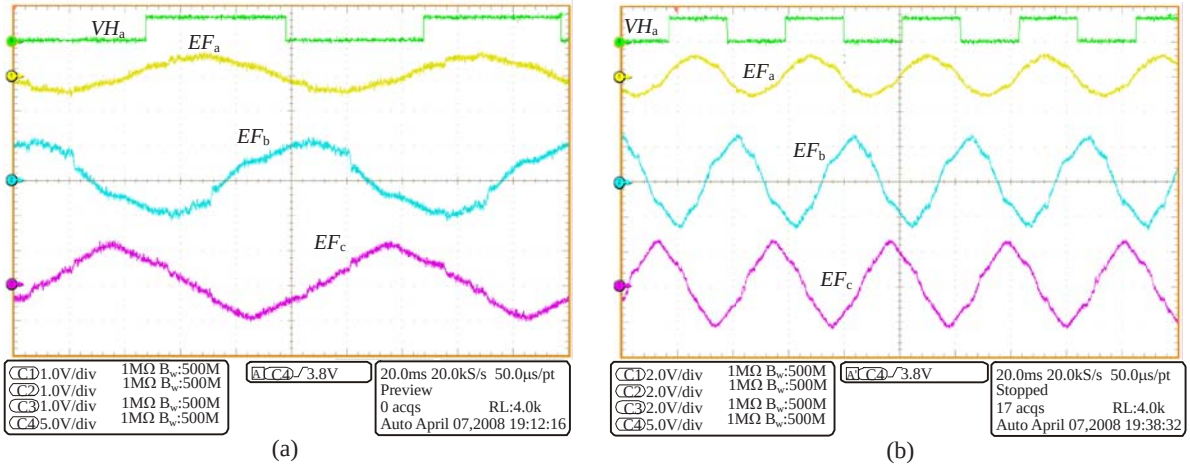

Fig.7 Error functions EF_a, EF_b and EF_c at 60 r/min (a) and 210 r/min (b)

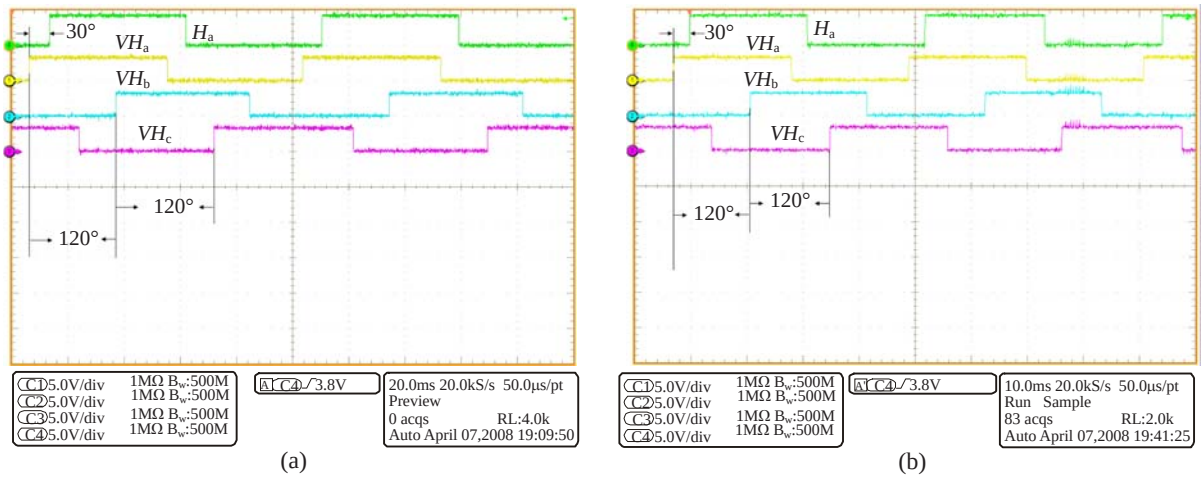

Fig.8 Developed virtual Hall sensor signals at 60 r/min (a) and 210 r/min (b)

commutation instants through software in this study (The 30° phase delay can also be created via fixed shift circuits, however, the accuracy will be decreased in such case).

Except the voltage measurement errors, phase delay of filters is the main source of the error in the developed sensorless method. As mentioned earlier it is at most 4° at 250 r/min and is negligible. Moreover, load torque does not make any error, because developed EFs around their zero crossings directly show the phase back-EMF voltage behavior. Experimental results show that the developed sensorless method can be started at 25 r/min for the employed BLDC motor.

In Fig.9, current waveforms under different loads and conditions are shown. The current scale of current transducers is 6. The motor is started in an open-loop scheme. Firstly, the motor is locked in mode II for a duration of 0.25 s. Then open-loop control is applied in the next four modes and then the virtual position signals are used for sensorless control algorithm. In Fig.9b, the current waveforms are shown while the load increases. Figs.9c and 9d show the current waveforms under 50% full load and at 60 and 160 r/min, respectively. The estimation error of the position signal is negligible and the current waveforms have little glitches. At high speeds, the back-EMF voltage of phase C affects the phase currents and causes a bit disturbance. Using the developed sensorless algorithm, current commutation is well done and the DPC control leads to rectangular phase currents.

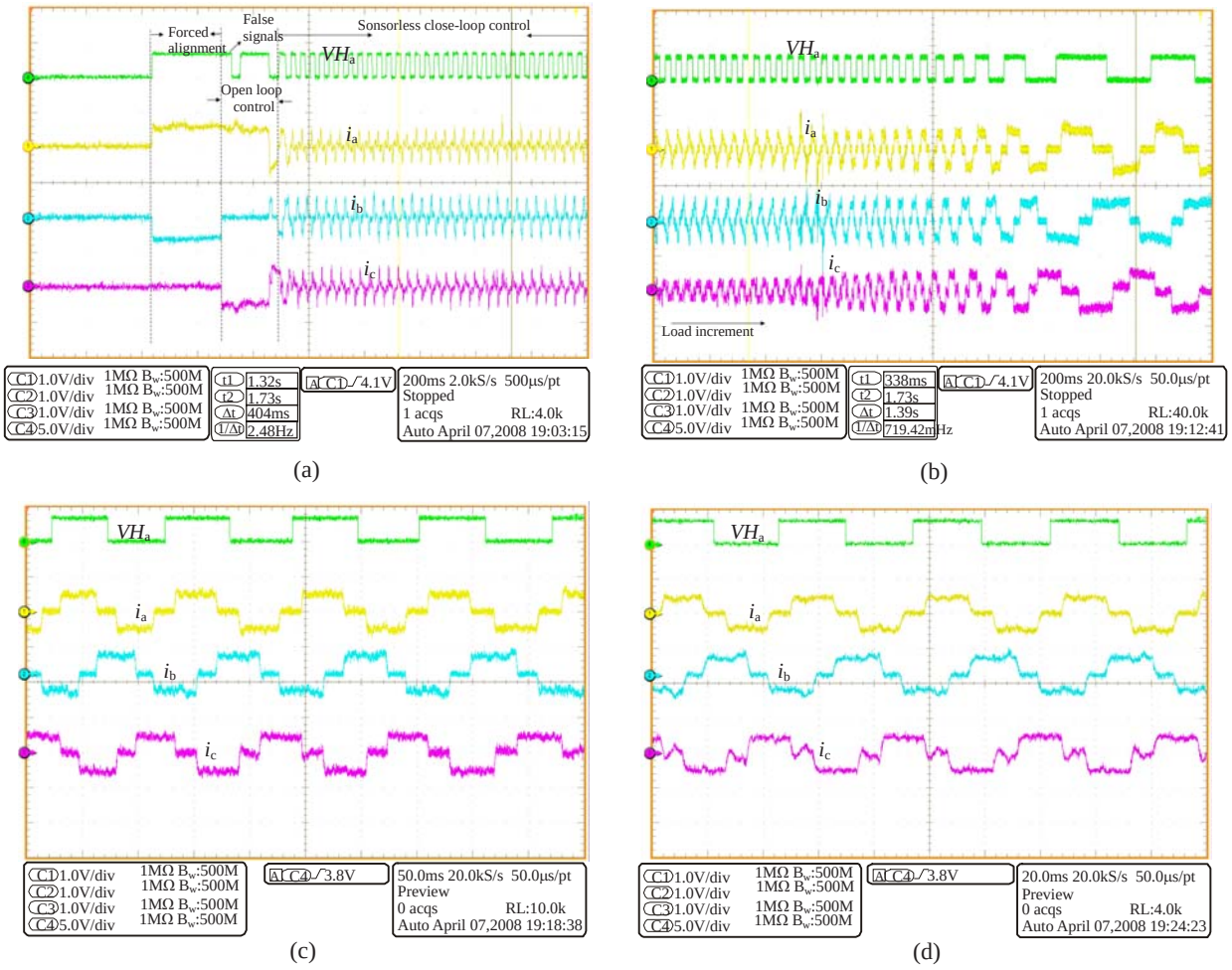

Fig.9 Phase current waveforms using virtual position signals motor startup (a), load torque change (b), at speed of 60 r/min under 50% full load (c), and at speed of 160 r/min under 50% full load (d)

CONCLUSION

A low-cost BLDC motor drive is introduced in this study. Cost saving is achieved by reducing the number of inverter switches and also elimination of the position Hall Effect sensors. The DPC control technique is used for the four-switch converter, which leads to the same characteristics as the six-switch converter. For current commutation, virtual Hall signals are made by a novel sensorless method using the EFs that are calculated from measured terminal voltages of phases A and B. Virtual Hall sensors are obtained from the detection of the proposed functions. The validity of the presented sensorless method is shown via simulations. Finally, the analysis and simulation results are verified by experimental results. The proposed method has several advantages as follows:

(1) Six commutation points are detected for four-switch inverter drive. Therefore, extra phase shifting is not required.

(2) Developed virtual Hall sensor signals are 30° before their corresponding commutation instants. Therefore, there is enough time to employ the effective methods for compensating the estimation errors and commutation torque ripple.

(3) Developed error functions have smooth transitions around zero level rather than other sensorless methods for four-switch BLDC motor drive. Therefore, the error of zero crossing detection is reduced.

(4) Since the amplitude of the EFs is larger than those of the phase voltage or even line voltages, a lower open-loop starting speed can be achieved.

References

Acarnley, P.P., Watson, J.F., 2006. Review of position-sensorless operation of brushless permanent-magnet machines. *IEEE Trans. Ind. Electron.*, **53**(2):352-362. [doi:10.1109/TIE.2006.870868]

Halvaei Niasar, A., 2007. Sensorless Control of Four-Switch, Three-phase Brushless DC Motor Drives for Low-cost Applications. PhD Thesis, Iran University of Science and Technology, Tehran, Iran.

Halvaei Niasar, A., Moghbelli, H., Vahedi, A., 2007. A Novel Sensorless Control Method for Four-switch, Brushless DC Motor Drive Without Using Any 30 Degree Phase Shifter. Proc. IEEE Int. Conf. on Electrical Machines and Systems, p.408-413. [doi:10.1109/ICEMS.2007.4411998]

Jahnson, J.P., Ehsani, M., Guzelaunler, Y., 1999. Review of Sensorless Methods for Brushless DC. Proc. IEEE IAS Annual Meeting Conf., **1**:143-150. [doi:10.1109/IAS.1999.799944]

Lee, B.K., Kim, T.H., Ehsani, M., 2003. On the feasibility of four-switch three-phase BLDC motor drives for low cost commercial applications: topology and control. *IEEE Trans. Power Electron.*, **18**(1):164-172. [doi:10.1109/TPEL.2002.807125]

Li, Q., Lin, M.Y., Hu, M.Q., Gu, W.G., 2006. Research on Filters for Back EMF Zero-crossing Detecting in Sensorless BLDC Motor Drives. Proc. IEEE Int. Conf. on Industrial Technology, **3**:1899-1905.

Lin, C.T., Hung, C.W., Liu, C.W., 2008. Sensorless control for four-switch three-phase brushless DC motor drives. *IEEE Trans. Power Electron.*, **23**(1):438-444. [doi:10.1109/TPEL.2007.911782]

Pillay, P., Krishnan, R., 1989. Modeling, simulation, and analysis of permanent-magnet motor drives, II: The brushless DC motor drive. *IEEE Trans. Ind. Appl.*, **25**(2):274-279. [doi:10.1109/28.25542]

Shao, J., Nolan, D., 2002. A Novel Direct Back EMF Detection for Sensorless Brushless DC (BLDC) Motor Drives. Proc. IEEE Applied Power Electronics Conf. and Exposition, **1**:33-37. [doi:10.1109/APEC.2002.989224]

Su, G.J., McKeever, W., 2004. Low-cost sensorless control of brushless DC motors with improved speed range. *IEEE Trans. Power Electron.*, **19**(2):296-302. [doi:10.1109/TPEL.2003.823174]

Texas Instruments, 2001. TMS320LFLC240xA DSP Controllers Reference Guide—System and Peripherals. No. SPRU357B.

Wang, C., Sung, G., Fang, K., Tseng, S., 2007. A Low-power Sensorless Inverter Controller of Brushless DC Motors. Proc. IEEE Int. Symp. on Circuits and Systems, p.2435-2438. [doi:10.1109/ISCAS.2007.378612]

Zhou, G., Wu, Z., Ying, J., 2005. Improved Sensorless Brushless DC Motor Drive. Proc. IEEE Power Electronics Specialists Conf., p.1353-1357. [doi:10.1109/PESC.2005.1581805]